===== **GEOCHEMISTRY** =====

Phase Relationships and Distribution of S, Fe, Co, Ni, Re, Os, and Pt between Metal and Sulfide Melts in the Basalt—Fe—FeS—C System at 1400°C and 4 GPa

N. S. Gorbachev[a],*, **Corresponding Member of the RAS Yu. B. Shapovalov[a], A. V. Kostyuk[a], P. N. Gorbachev[a], and A. N. Nekrasov[a]**

Abstract—The immiscibility of a Fe—FeS—C melt into Fe-metal (Mc) and Fe-sulfide (Ms) liquids has been studied in the basalt—Fe—FeS—C system at 4 GPa and 1400°C. The partition (D) and distribution (Kd) coefficients of S, Fe, Co, Ni, Re, Os, and Pt between the Mc and Ms melts are determined. The partition coefficients D served as indicators of the siderophilic and chalcophilic properties of each element, and Kd characterized their interelemental ratios during fractionation. In the Fe—Os—Co—Re series with D > 1, siderophilic properties prevail, which increase with increasing values of the partition coefficients: 1.2–1.5–1.6–12.6. In the Ni—Pt—S series with D < 1, chalcophilic properties prevail, which increase with decreasing D: 0.9–0.6–0.1. The values of the distribution coefficients Kd Re/Os (8.4) and Pt/Os (0.4) indicate the fractionation of Re and Pt relative to Os, with enrichment of rhenium in a metallic melt and platinum in a sulfide melt and a shift in the fractionation of the Re/Os and Pt/Os relations and related systems of ^{187}Re/^{187}Os and ^{190}Pt/^{186}Os isotopes. The genetic relationship of magmatic sulfide mineralization in intrusive of the Upper Norilsk (ore-bearing) and Lower Norilsk (ore-free) types with metal—sulfide immiscibility of sulfide magma is evidenced by the similarity of the Re/Os ratio in the Upper Norilsk intrusive with the ratio in the Ms component, and in the Lower Norilsk intrusive with the Mc component.

Melting and phase relationships in the basalt—Fe—S—C system are of interest because, unlike the binary Fe—S and Fe—C systems with eutectic relationships between Fe-metal and Fe-sulfide (or Fe-carbide) phases with complete miscibility among their melts, the Fe—S—C system demonstrates layering of the sulfide melt into Fe-metal (Mc) and Fe-sulfide (Ms) melts, which are immiscible with the silicate melt (L) [1–3].

Signs of the immiscibility of Mc and Ms melts were observed in basaltic glasses from the effusive rocks of Disko Island, Greenland [4]. The experimental immiscibility of Mc and Ms melts and its role in the processes of early differentiation of meteorites, planets, and their satellites were discussed in [5, 6]. Later on, various aspects of metal-sulfide liquation in the Fe—S—C system and their significance in geological processes were studied in a series of experimental works [7–10].

A sensitive indicator of these processes is the distribution of Re, Os, Pt, Ni, and Co between the metallic (Mc) and sulfide (Ms) melts. Geochemically, these elements combine double properties: siderophile and chalcophile. At the experimental parameters in metallic-silicate melt (L) equilibria, these elements are effectively concentrated in the metallic melt, with the partition coefficients between the metallic and silicate melts, D Mc/L, reaching three or more orders of magnitude [11–13]. In the sulfide–silicate melt equilibria, these elements also have chalcophile properties with D Ms/L reaching 3–5 orders of magnitude [14–17]. Of geochemical interest is the question which properties, siderophile or chalcophile, prevail for each of these elements. The formation of metallic and sulfide melts in the Fe—S—C system makes it possible to study the distribution of Co, Ni, Re, Os, and Pt between the Mc and Ms melts in one experiment, enabling the assessment of chalcophile and siderophile properties of each of these elements based on the partition coefficient D^i Mc/Ms = C^i (Mc)/C^i (Ms) between the Mc

[a] *Korzhinskii Institute of Experimental Mineralogy,*
Russian Academy of Sciences, Chernogolovka, Moscow oblast,
142432 Russia
*e-mail: gor@iem.ac.ru

Table 1. Representative chemical compositions (wt %) of the coexisting phases of the silicate part

Oxide/Phase	Grt	Cpx	L_1	L_2	Mk basalt
SiO_2	38.87 ± 0.50	50.07 ± 0.50	41.73 ± 1.70	42.14 ± 0.64	50.08
TiO_2	1.05 ± 0.31	<DL	2.54 ± 0.22	1.55 ± 0.15	1.85
Al_2O_3	21.55 ± 0.95	8.45 ± 0.67	8.91 ± 0.50	9.94 ± 0.19	14.53
FeO	20.95 ± 1.66	13.07 ± 1.38	33.96 ± 1.46	29.46 ± 0.65	14.05
MgO	8.38 ± 1.45	10.07 ± 0.22	1.85 ± 0.33	4.25 ± 0.20	5.86
CaO	8.45 ± 0.29	15.32 ± 0.42	4.9 ± 0.12	8.29 ± 0.24	10.41
Na_2O	<DL	2.29 ± 0.31	3.67 ± 0.98	2.76 ± 0.12	2.5
K_2O	<DL	<DL	0.6 ± 0.01	0.73 ± 0.18	0.72
Sum	99.25	99.27	98.09	99.12	100.00

and Ms melts, where C^i is the concentration of each element in the Mc or Ms melts.

For this purpose, Fe, Co, Ni, Re, Os, Pt, and S were distributed between Mc and Ms melts in the basalt−Fe−FeS−C system during two experiments at $P = 4$ GPa and $T = 1400°C$ on an anvil-with-hole apparatus (NL-40) using a multiampoule quenching technique [18]. The temperature was measured with a Pt30Rh/Pt6Rh thermocouple, and the pressure was calibrated at high temperatures by the quartz−coesite equilibrium. The accuracy of the temperature and pressure measurements is estimated at ±10°C and ±1 kbar [19]. The initial composition consisted of silicate and ore fractions in the ratio of 1 : 2. The silicate fraction included silicate glass from the magnesium basalt of the Mokulaevskaya (mk) formation of the Norilsk region and had the following composition (wt %): 50.02 of SiO_2; 1.85 of TiO_2; 14.51 of Al_2O_3; 14.03 of FeO; 0.20 of MnO; 5.85 of MgO; 10.40 of CaO; 2.50 of Na_2O; and 0.72 of K_2O. The ore fraction consisted of a mixture of pyrrhotine with the following composition (wt %): Fe = 57.06 and S = 34.60 ($Fe_{0.94}S_{1.0}$) synthesized by the method of pyrosynthesis (58 wt %), a reagent of chemically pure metallic Fe (36 wt %) and technical carbon (6 wt %, grade P-803). To clarify the behavior of trace elements, 0.5 wt % of each metallic Re, Os, and Pt were added to the sample.

The experiments were conducted by the "sandwich" technique: the silicate and ore fractions were loaded into a graphite ampoule layer by layer in the "ore−silicate−ore" sequence. The graphite ampoule was placed in a Pt ampoule with $d = 5$ mm, which was hermetically sealed. After the experiment, the ampoule was cut transversely and pressed into polystyrene. The polished quenched specimens were studied by means of a Tescan Vega II XMU digital scanning microscope equipped with an energy-dispersive X-ray spectrometer (EDS) with an INCA Energy 450 semiconductor Si (Li) detector and an INCA Wave 700 wavelength-dispersive spectrometer (WDS) in the Energy Plus mode. The wavelength-dispersive spectrometer was employed to analyze the minimum concentrations of Re, Os, and Pt using pure metals as standards. The studies were performed at an accelerating voltage of 20 kV, and the current of absorbed electrons on the Faraday cylinder was 82 nA. The spectrum accumulation time on EDS was 200 s. For WDS data acquisition, the standardization was 40 s; the spectrum accumulation time for S, Fe, Ni, and Co was 40 s; for Re, Pt, and Os it was 100 s. Under these conditions, the detection limits with a probability of 99.73% are equal to 3σ. The results of the X-ray spectral microanalysis were processed using the INCA software ver. 4.06 with subsequent recalculation of the obtained results using a software package developed at the Korzhinskii Institute of Experimental Mineralogy, Russian Academy of Sciences.

The features of the phase and chemical composition of the quenched samples are presented in Table 1 and Figs. 1−3.

The silicate fraction is represented by the association of Grt + Cpx and silicate glass, a quenched silicate melt in the form of intergranular and continuous (injection) precipitations formations (Fig. 1, Table 1). The intergranular melt (L_1) occurs between Grt and Cpx in the silicate part of the specimen. Most of the silicate melt (L_2) separated from the Grt−Cpx−restite, forming clusters in the ore part of the sample. During migration and intrusion, the silicate melt captured individual portions of sulfides. The concentrations of siderophile elements in the silicate component of the quenched samples were below the detection limit (0.1 wt %) on the microprobe.

The idiomorphic crystals of garnet, from 10 to 30 μm in size, having an almandine−pyrope−grossular composition, contain ≤1 wt % of TiO_2 and Cr_2O_3. In terms of the main mineral-forming components SiO_2, Al_2O_3, MgO, CaO, and FeO, the garnets are homogeneous. There is slight zoning, manifesting itself in the change in TiO_2 contents (from 1.2 to 0.6 wt %) from the center to the rim of the grain. Clinopyroxenes are represented by tabular-shaped diopside−hedenbergite
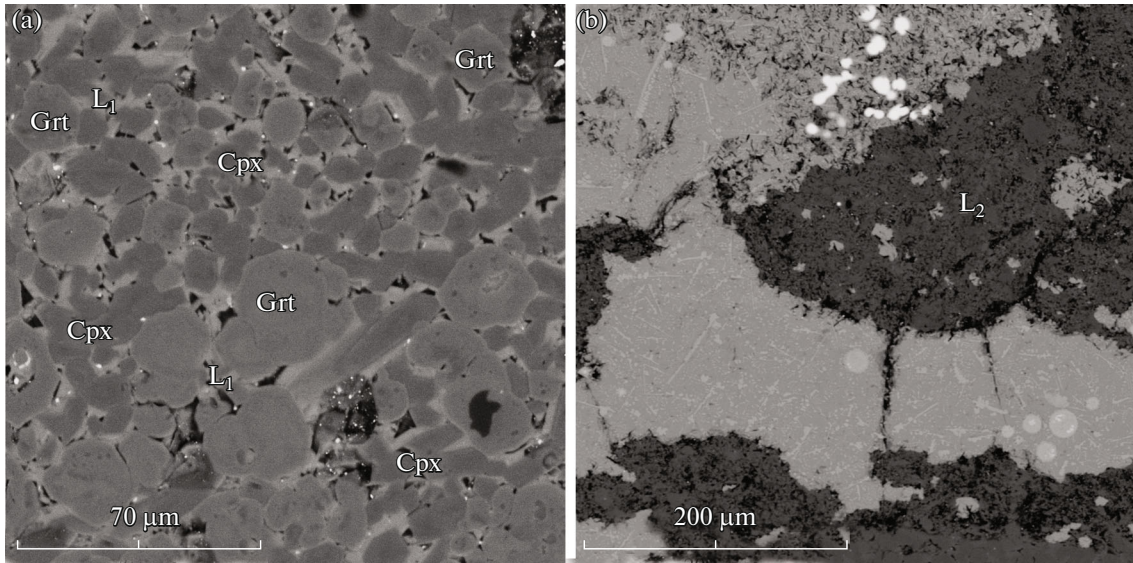
Fig. 1. BSE micrographs of the silicate part of the experimental sample: (a) Grt−Cpx matrix with intergranular glass (L_1); (b) massive glass precipitations from the injection melt (L_2) in the ore part.

precipitations $(Ca_{0.6}Mg_{0.5}Fe_{0.4})(Al_{0.3}Na_{0.1})Si_2O_6$ from 10 to 50 μm in size (Table 1).

A distinctive feature of the intergranular glass is the increased content of FeO (up to 34 wt %) and alkalis ($Na_2O + K_2O$ up to 5 wt %), as well as decreased contents of CaO (up to 5 wt %) and MgO (up to 2 wt %). The composition of the melts corresponds to alkaline ferrobasalts. Like the intergranular melts, the injection melts are characterized by high contents of FeO (up to 29 wt %). Compared to the melts L_1, the injection melts L_2 are characterized by higher contents of MgO, up to 4 wt %, alkalis ($Na_2O + K_2O$ up to 4 wt %), CaO

(up to 8.5 wt %), and low TiO_2 (1.6 wt %) (Table 1). Unlike the initial basalt, the intergranular and injection glass have abnormally high content of FeO (up to 34 wt %), low MgO (up to 2 wt %), low CaO (up to 5 wt %), increased contents of Na_2O (up to 3.7 wt %) and TiO_2 (2.5 wt %), and decreased contents of K_2O (<0.3 wt %). The contents of Ni, Re, Os, and Pt in the glasses vary significantly from 0.1 to 1.5 wt %. Such high concentrations are related to microinclusions of ore phases enriched with these elements in the silicate glass.
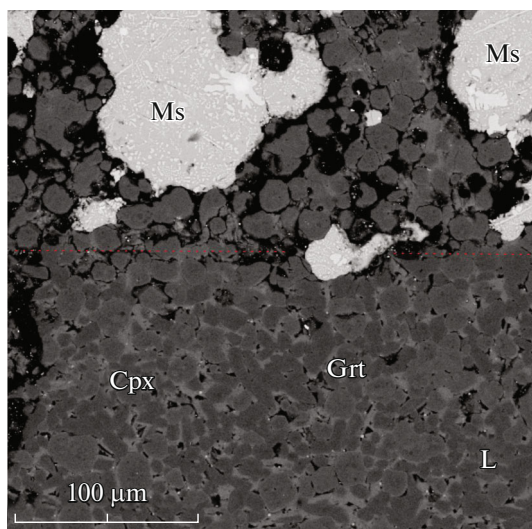
Fig. 2. Microimage of the Grt−Cpx restite contact zone with isolated sulfide inclusions (BSE micrograph).
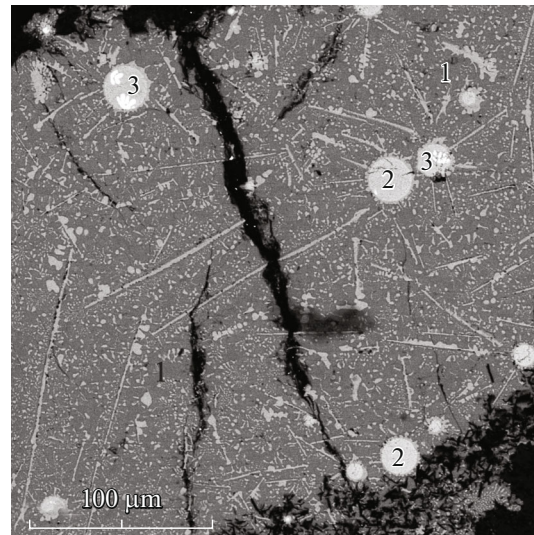
Fig. 3. Microimage of massive sulfides with inclusions of monophase and polyphase Fe-metal globules (BSE micrograph): 1, quenching sulfide matrix; 2, monophase Fe-metal globules; 3, polyphase Fe-metal globules.

Table 2. Concentrations of S, Fe, Co, Ni, Re, Os, and Pt (wt %) in the Mc and Ms phases, partition coefficients between the Mc and Ms melts

Element	Mc, $n = 21$	Ms, $n = 16$	D Mc/Ms
S	1.45 ± 0.49	26.68 ± 0.56	0.05
Fe	88.18 ± 1.69	72.18 ± 0.80	1.22
Ni	0.37 ± 0.15	0.40 ± 0.12	0.92
Re	9.96 ± 1.49	0.79 ± 0.45	12.64
Os	0.54 ± 0.16	0.36 ± 0.06	1.51
Pt	0.39 ± 0.22	0.63 ± 0.10	0.62
Co	1.28 ± 0.16	0.80 ± 0.18	1.6

In the silicate fraction, isolated precipitations of sulfides are found in the Grt–Cpx–restite contact zone (Fig. 2) as xenomorphic polyphase precipitations with a matrix having pyrrhotite composition, up to 100 μm in size, and containing up to 0.6 wt % of Pt and 0.3 wt % of Ni, Os, and Re. The sulfide matrix contains inclusions of the Fe-metal phase up to 10 μm in size, with 84–95 wt % of Fe, up to 7 wt % of Re, and 0.4–0.7 wt % of Ni, Os, and Pt. The carbon concentration, estimated by complementing the sum of the analysis to 100%, is 3.7–4.7 wt %.

The ore fraction of the quenched samples is represented by interlayers of massive sulfides, the matrix of which contains needle-shaped microinclusions of the quenching Fe-metal phase, almost free of impurities, and has globule inclusions of the Fe-metal phase, up to 20 μm in size, either monophase, without inclusions, and polyphase, with Fe–Re inclusions (Fig. 3).

Monophase Fe-metal globules are characterized by high contents of Fe (87–89 wt %) and Re (7–10 wt %) and contain up to 1.3 wt % of Co and ~0.3–0.6 wt % of Ni, Os, and Pt. The reduced sums of microprobe analyses of the Fe-metal globules indicate solubility of up to 4 wt % of carbon in them (Fig. 3).

At rhenium contents greater than 10 wt %, the metallic melt is saturated with rhenium, which is accompanied by the precipitation of the Fe–Re phase and the formation of polyphase globules.

Polyphase Fe-metal globules. The matrix of polyphase globules with a rhenium concentration of ~7 wt % contains oval-shaped inclusions of the Fe–Re-phase, with up to 26 wt % of Re (Fig. 3).

Distribution of S, Fe, Co, Ni, Re, Os, and Pt between Metallic and Sulfide Melts and Evaluation of Chalcophile and Siderophile Properties of Each Element

Table 2 presents the representative chemical compositions of coexisting sulfide and metallic melts and the partition coefficients D of ore elements between them.

The indicator of siderophile and chalcophile properties, that is, the relative affinity of an element for the Mc and Ms phases, is the partition coefficients of each element between the metallic (Mc) and sulfide (Ms) melts coexisting in the Fe–S–C system, which are expressed as the ratio of the concentrations (C) of this element in the Mc melt to its concentration in the Ms melt: D (Mc/Ms) = C (Mc)/C (Ms). For the elements with D (Mc/Ms) = 1, the siderophile and chalcophile properties manifest themselves equally. For the elements with D (Mc/Ms) > 1, siderophile properties dominate, and with D (Mc/Ms) < 1, chalcophile properties dominate. The greater the deviation of D (Mc/Ms) from 1, the stronger the siderophile properties (at D > 1) or chalcophile properties (at D < 1).

The data presented in Table 2 show that, for Fe, Co, Re, and Os, the partition coefficients D > 1; consequently, for each of these elements, siderophile properties dominate over chalcophile properties. The siderophile properties increase at an increase in D in the sequence Fe < Os < Co < Re. Re has the strongest affinity in this series for the Fe-metal phase (siderophilicity), with D = 12.64. The other elements in the series Fe, Os, and Co are characterized by less contrasting differences in the siderophile and chalcophile properties with low values (<2) of the partition coefficients. The significant concentrations of sulfur in the metallic melt indicate its solubility in Fe-metallic melts.

Chalcophile properties are dominant in the series of elements S, Ni, and Pt with D < 1, which increase at a decrease in the partition coefficients between the metallic and sulfide melts in the sequence of Ni < Pt < S. The increase in chalcophilicity is characterized by partition coefficients between the metallic and sulfide melts, which decrease in the sequence of 0.92–0.62–0.05. Ni and Pt with low values of D close to 1 show less contrasting differences in chalcophile and siderophile properties compared to S.

The efficiency of the fractionation of each element during the distribution between metallic and sulfide melts is characterized by the absolute values of D (Mc/Ms). The greater these values deviate from 1, the stronger the siderophile properties (at D > 1) or chalcophile properties (at D < 1). The relatively low values of the partition coefficients for Co, Ni, Os, and Pt indicate a moderate fractionation during the distribution between the Mc and Ms melts, as well as small variations in their ratios in the coexisting Mc and Ms melts. At the same time, the high values of D for Re compared to D for Os and Pt indicate effective fractionation of Re relative to Os and Pt due to redistribution into the metallic melt, which will lead to a decrease in the Re/Os and Re/Pt ratios in the coexisting Fe-sulfide melt.

Thus, S, Fe, Co, Ni, Re, Os, and Pt, which have strong siderophile properties (in equilibria of metallic and silicate melts) and chalcophile properties (in equi-

libria of sulfide and silicate melts), based on the values of the partition coefficients between the coexisting metallic and sulfide melts, show that, for Fe, Co, Re, and Os, the siderophile properties prevail over the chalcophile ones, increasing at an increase in the partition coefficient in the sequence of Fe < Os < Co < Re. In contrast, for S, Ni, and Pt, the chalcophile properties dominate over the siderophile ones, increasing upon a decrease in the partition coefficients in the sequence of Ni < Pt < S.

FUNDING

CONFLICT OF INTEREST

The authors of this work declare that they have no conflicts of interest.

REFERENCES

1. R. Brett and P. M. Bell, Earth Planet. Sci. Lett. **6** (6), 479−482 (1969).
https://doi.org/10.1016/0012-821X(69)90119-8

2. O. A. Bannykh, P. B. Budberg, and S. P. Alisova, *State Diagrams for Double and Multicomponent Iron-Based Systems* (Metallurgiya, Moscow, 1986) [in Russian].

3. V. Raghavan, J. Alloy Phase Diagrams **4** (2), 133−142 (1988).

4. A. K. Pedersen, Contrib. Mineral. Petrol. **69** (4), 397−407 (1979).

5. N. S. Gorbachev and E. G. Osadchii, Dokl. Akad. Nauk SSSR **255** (3), 693−697 (1980).

6. N. S. Gorbachev, E. G. Osadchii, and G. V. Baryshnikova, in *Proc. Lunar and Planetary Science Conf.* (Houston, 1980), Vol. 11, pp. 348−350.

7. A. A. Marakushev, Yu. B. Shapovalov, N. G. Zinov'eva, et al., Dokl. Akad. Nauk **345** (6), 797−801 (1995).

8. R. Dasgupta, A. Buono, G. Whelan, et al., Geochim. Cosmochim. Acta **73** (21), 6678−6691 (2009). https://doi.org/10.1016/j.gca.2009.08.001

9. L. A. Hayden, J. A. Van Orman, W. F. McDonough, et al., Geochim. Cosmochim. Acta **75** (21), 6570−6583 (2011). https://doi.org/10.1016/j.gca.2011.08.036

10. N. S. Gorbachev, A. V. Kostyuk, P. N. Gorbachev, et al., Experim. Geosci. **27** (1), 42−44 (2021).

11. J. M. Brenan, N. R. Bennett, and Z. Zajacz, Rev. Mineral. Geochem. **81** (1), 1−87 (2016). https://doi.org/10.2138/rmg.2016.81.1

12. J. Siebert, A. Corgne, and F. J. Ryerson, Geochim. Cosmochim. Acta **75**, 1451−1489 (2011). https://doi.org/10.1016/j.gca.2010.12.013

13. U. Mann, D. J. Frost, D. C. Rubie, et al., Geochim. Cosmochim. Acta **84**, 593−613 (2012). https://doi.org/10.1016/j.gca.2012.01.026

14. A. J. Naldrett, *Magmatic Sulfide Deposits* (Oxford, 1989), No. 14.

15. M. E. Fleet, J. H. Crocket, and W. E. Stone, Geochim. Cosmochim. Acta **60** (13), 2397−2412 (1996). https://doi.org/10.1016/0016-7037(96)00100-7

16. E. S. Kiseeva and B. J. Wood, Earth Planet. Sci. Lett. **383**, 68−81 (2013). https://doi.org/10.1016/j.epsl.2013.09.034

17. J. E. Mungall and J. M. Brenan, Geochim. Cosmochim. Acta **125**, 265−269 (2014). https://doi.org/10.1016/j.gca.2013.10.002

18. N. S. Gorbachev, Int. Geol. Rev. **32** (8), 749−836 (1990).

19. Yu. A. Litvin, *Physicochemical Research of the Earth's Deep Matter Melting* (Nauka, Moscow, 1991) [in Russian].

Translated by L. Mukhortova